End-to-Side 혈관문합에서의 삼차원유동: 정상유동 및 맥류유동

김 영호

서울대학교 의공학과

Three-Dimensional Flow in an End-to-Side Vascular Anastomosis: Steady and Pulsatile Flow

Young H. Kim

Institute of Biomedical Engineering, Seoul National University

ABSTRACT

Three-dimensional steady and pulsatile flows in an end-to-side anastomosis were investigated using a finite difference method in order to understand the flow dynamics in the preferential development of distal anastomotic intimal hyperplasia or thrombosis. Steady flow results revealed that a double helical vortex was formed in the host artery and flow recirculations near tow and heel regions were limited due to the secondary flow. Oscillating wall shear stress with significant secondary flow might be the flow dynamic reason of developing intimal hyperplasia or thrombosis.

INTRODUCTION

Intimal hyperplasia or thrombosis have been found primarily at the distal anastomosis as a major source of failure in by-pass graft replacements. Important interactions between fluid dynamics and the chronic development of intimal hyperplasia have been suggested. Many investigators [1-5] have correlated intimal thickening or plaque development in the region of low and oscillating shear with flow separation. Clinical results [6,7] show that a preferred location for the development of hyperplasia is near the toe of the anastomosis and along the outer wall where the inlet stream strikes the wall.

In vitro flow visualization studies [8,9] on models of end-to-side anastomosis using dye injection or aluminum tracer particles have provided useful information on the flow dynamics in the anastomotic region. In vitro experiments were carried out using the laser Doppler anemometry, hot-film anemometry and photochromic tracer technique [10-12]. Simple two-dimensional steady flow simulations showed low shear stress distributions near the heel and toe region. It was also reported that smaller anastomotic junction angle is recommended in the distal end-to-side anastomosis in the hemodynamic point of view [13]. The secondary flow motion as well as the double helical vortex are very important in three-dimensional flow in an end-to-side anastomosis, but are not well described yet. Therefore, the aim of the present study is to investigate steady and pulsatile flows near the region of an end-to-side anastomosis using a finite difference method. This will provide valuable quantitative information relating abnormal flow dynamics with regions of anastomotic intimal hyperplasia or plaque development.

METHODS

A computational fluid dynamics software, FLUENT (FLUENT Inc., New Hampshire), was used to investigate the three-dimensional flow characteristics near the anastomosis. A graft of the same diameter of 6 mm as the host artery was anastomosed with a junction angle of 45^{0}, and the proximal end of the artery was assumed to be occluded. A non-uniform boundary-fitted structural grid distribution of 41×10×31 was used for the study.

For incompressible, Newtonian fluid, the governing equation for three-dimensional unsteady laminar flow can be expressed as:

$$\nabla \cdot \boldsymbol{u} = 0 \qquad (1)$$

$$\frac{\partial \boldsymbol{u}}{\partial t} + \boldsymbol{u} \cdot \nabla \boldsymbol{u} = -\nabla p + \frac{1}{Re} \nabla^2 \boldsymbol{u} \qquad (2)$$

where $\boldsymbol{u}$ are the velocities, p is the pressure and Re is the Reynolds number based on the vessel diameter. In order to solve the above partial differential equations, computational domain was discretized into a collection of control volumes and the differential equations are approximated by a set of algebraic equations. Patankar's SIMPLE procedure was introduced to solve the coupling of velocities and pressure.

The vessel wall was assumed to be rigid, and the density of 1.056 g/cm^3 and the dynamic viscosity of 3.5 cP were employed. The mean Reynolds number was chosen to be 510 for the steady flow simulation, representative of the peak values for flow in the femoral artery. Figure 1 shows the physiological pressure gradient wave form over a cardiac cycle which was used for the inlet boundary condition in pulsatile flow simulation.

RESULTS

To help the understanding of the results, the following specified locations in the vessel wall are introduced, as shown in Figure 2: aa' is the inner wall, bb' is 45° from the inner wall, cc' is the side wall, dd' is 45° from the outer wall and ee' is the outer wall. A, B, C and D represent specified cross-sections in the host artery.

Steady Flow

At the stagnation point along the outer wall (ee'), the flow stream splits into two parts with one stream moving in the direction of the outlet branch and the other stream moving in the direction of the occlusion. A limited flow separation was also found at toe region in the anastomotic junction. Flow recirculations distal to the toe region along the near wall, were limited due to the secondary flow. Figure 3 shows axial velocity profiles and secondary flow velocity vectors at specified cross-sections in the host artery. The axial velocity profile at the distal locations of the host artery became skewed towards the outer wall, as shown in cross-sections C and D at Figure 3. Secondary vortices in the distal host artery are very significant and their circumferential motion became maximum at the side wall (cc') and minimum at the outer wall (ee'). Fluid close to the wall in the anastomotic junction quickly turns around with this helical vortices, while fluid near the center line of the host artery accelerates as flow moves to the anastomotic junction. Fluid near the side wall (cc') is also get accelerated by this helical vortex, and then results in M-shaped axial velocity profile at 1.5D in the distal host artery. Figure 4 shows the streaklines describing the double helical vortex in the host artery.

Pulsatile Flow

Figure 5 describes velocity vector fields in the plane of symmetry at the following periods: systolic acceleration, t/t_p = 0.1, peak systole t/t_p = 0.15, systolic deceleration t/t_p = 0.3, reversed pressure gradient t/t_p = 0.4 and diastole t/t_p = 0.7. At t/t_p = 0.1, a small vortex is present below the heel region near the outer wall (ee').and axial velocity profiles become skewed toward the outer wall (ee') in the downstream host artery. During peak systole t/t_p = 0.15, axial velocity profiles become skewed more toward the outer wall and the vortex near the outer wall becomes even stronger. At this time, axial velocity components at C and D significantly increase due to the secondary flow motion. At t/t_p = 0.3, a only a small amount of forward flow was observed and the vortex near the heel region moves downstream and toward the graft. A widespread flow recirculation is also shown distal to the toe region. However, small amount of forward flow maintains near the outer wall (ee'), as shown in Figure 5(c). At t/t_p = 0.4, due to the negative pressure gradient, reversed flow occurred from the host artery to the graft and the stagnation point on the outer wall disappeared. Flow close to the outer wall near the anastomosis remained relatively stagnant. Velocity profiles in the graft also become skewed toward the near wall and velocities near the anastomotic junction are relatively small. At t/t_p = 0.7, only a small amount of flow was observed and some forward flow was found close to inner and outer walls. Flow in the graft turns slowly into the proximal occlusion along the outer wall (ee').

DISCUSSION

To date, the exact etiology of the anastomotic neointimal hyperplasia and thrombosis is unknown. The greatest amount of intimal thickening in a distal graft anastomosis occurred at localized area of low or highly oscillating wall shear stress such as the toe, heel and near the stagnation point. Fluid particles reside in the recirculation zone for a relatively long time, which might result in a higher potential for the mass transfer across the intimal layer to create intimal hyperplasia. Stresses in the high wall shear regions may also induce primary intimal hyperplasia in the low shear regions, by causing endothelial cells in the high wall shear regions to secrete growth factors that are transported and to accumulate in the low flow regions. Fry [14] suggested that deformation, swelling, and eventual erosion of the endothelium might occur at sites where the local shear stress is relatively high. Giddens et al. [15] recently reported that the determining factor of the intimal hyperplasia may be the maximum wall shear experienced during the cycle, regardless of directions and not simply the mean shear value. It is now recognized that the arterial diameter in a variety of mammalian species, including humans, responds to long term changes in flow conditions such that the mean wall shear stress is maintained in a range from 10 to 20 dyne/cm^2 [16,17], leading to the conclusion that arteries adapt to fluid dynamic wall shear stress in a very sensitive manner. Secondary flow in the anastomosis region is very important and large circumferential wall shear stresses occurred along the arterial wall. These high circumferential wall shear stresses might deform fibrous tissue on the vessel wall and in turn damage the intimal layer by acting with axial wall shear stresses.

CONCLUSION

Double helical vortex and the resulting secondary motions were found to be very important in flow across the end-to-side anastomosis. Flow recirculations near the toe and heel regions were limited due to the secondary flow. Pulsatile flow results revealed that oscillating wall shear stresses were observed at regions such as heel, toe and the stagnation point where intimal hyperplasia or thrombosis is popular. Large circumferential wall shear stress near the anastomosis might also be one of the

hemodynamic sources of graft implantation failure.

REFERENCES

1. Caro CG et al.: Proc R Soc Lond B117:109-159, 1971.
2. Rittgers SE et al.: Circ Res 42:792-801, 1978.
3. Bassiouny HS and Leiber BB: Surgical Forum: Cong Am Coll Surg Oct, 328-329, 1988.
4. Kim YH et al.: Ann Biomedical Eng 21, 311-320, 1993.
5. Ku DN et al.: Arteriosclerosis 5:293-302, 1985.
6. Logerfo FW et al.: Arch Surg 114:1369-1373, 1979.
7. Sottiurai VS et al.: Ann Vasc Surg 1:26-33, 1989.
8. Crawford HM et al.: Arch Surg 115:1280-1284, 1980.
9. Watts KC et al.: J Biomech 19:491-499, 1986.
10. Keynton RS et al.: J Biomech Eng 113: 458-463, 1991.
11. Kim YH and Chandran KB: Biorheology 30:117-130, 1993.
12. Ojha M et al.: J Vasc Surg 12:747-753, 1990.
13. Chandran KB and Kim YH: IEEE EMB (In press).
14. Fry DL: Circ Res 22:165-197, 1968.
15. Giddens DP et al.: Third U.S.A.- China - Japan Conference on Biomechanics 66-67, 1991.
16. Zarins CK et al.: J Vasc Surg 5:413-420, 1987.
17. Giddens DP et al.: Appl Mech Rev 43:S98-S102, 1990.

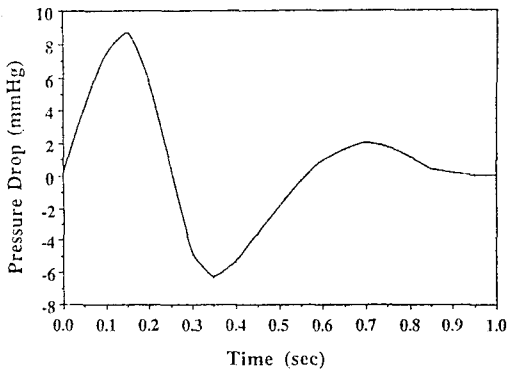

Figure 1. Pressure gradient wave form for the pulsatile flow simulation.

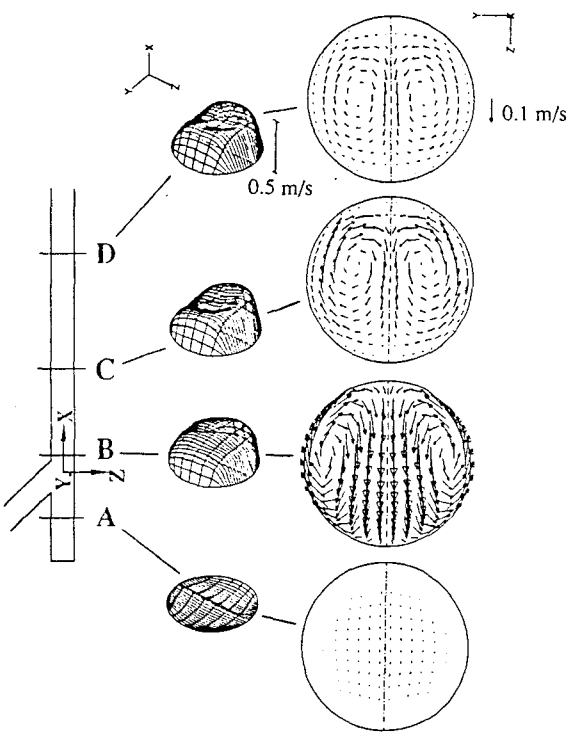

Figure 3. Axial velocity profiles and secondary velocity vectors at specified locations of the host artery.

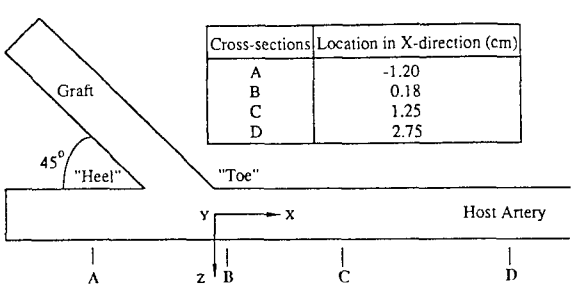

Cross-sections	Location in X-direction (cm)
A	-1.20
B	0.18
C	1.25
D	2.75

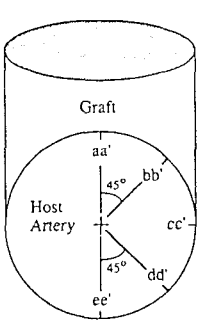

Figure 2. Schematic of the end-to-side anastomosis.

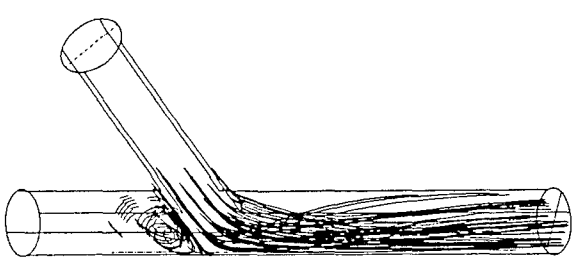

Figure 4. Streaklines for the steady flow

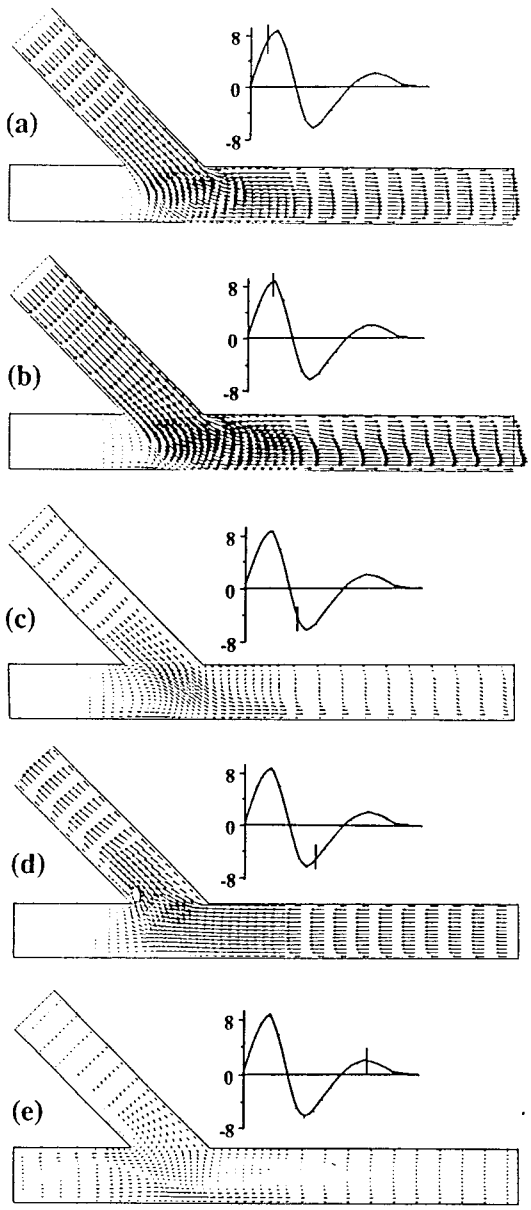

Figure 5. Velocity vector fields in the plane of symmetry at various time periods.